Localization of a Substrate Binding Site on the FeMo-Cofactor in Nitrogenase: Trapping Propargyl Alcohol with an α-70-Substituted MoFe Protein†

Paul M. C. Benton,‡ Mikhail Laryukhin,§ Suzanne M. Mayer,|| Brian M. Hoffman,*,§ Dennis R. Dean,*,|| and Lance C. Seefeldt*,‡

Department of Chemistry and Biochemistry, Utah State University, Logan, Utah 84322, Department of Chemistry, Northwestern University, Evanston, Illinois 60208, and Department of Biochemistry, Virginia Tech, Blacksburg, Virginia 24061

Received April 14, 2003; Revised Manuscript Received May 28, 2003

ABSTRACT: Substitution of the MoFe protein α-70^{Val} residue with Ala or Gly expands the substrate range of nitrogenase, allowing the reduction of larger alkynes, including propargyl alcohol (HC≡CCH$_2$OH). Herein, we report characterization of the α-70$^{Val→Ala}$ MoFe protein with propargyl alcohol trapped at the active site. The α-70^{Ala} variant MoFe protein was rapidly frozen during reduction of propargyl alcohol, resulting in the conversion of the resting-state FeMo-cofactor EPR signal ($S = {}^3/_2$ and $g = [4.41, 3.60, 2.00]$) to a new state ($S = {}^1/_2$ and $g = [2.123, 1.998, 1.986]$). This EPR signal of the new state increased in intensity with increasing propargyl alcohol concentration, consistent with the binding of a single substrate. The EPR signal of the propargyl alcohol state showed temperature and microwave power dependencies markedly different from those of the classic FeMo-cofactor EPR signal, consistent with the difference in spin. The new state is analogous to that induced by the binding of the inhibitor CO ("lo CO" state) to FeMo-cofactor in the wild-type MoFe protein. The ^{13}C ENDOR spectrum of the α-70^{Ala} MoFe protein with trapped ^{13}C-labeled propargyl alcohol exhibited three well-resolved ^{13}C doublets centered at the ^{13}C Larmor frequency with isotropic hyperfine couplings of ∼3.2, ∼1.4, and ∼0.7 MHz, indicating that the alcohol (or a fragment) is coordinated to the cofactor. The results presented here localize the binding site of propargyl alcohol to one [4Fe-4S] face of FeMo-cofactor and indicate roles for the α-70^{Val} residue in controlling FeMo-cofactor reactivity.

The binding and reduction of N_2 or alternative substrates (e.g., acetylene) by Mo-dependent nitrogenases occurs at an FeMo-cofactor[1] contained in the MoFe protein (*1*−*3*). X-ray structures of MoFe proteins from several microorganisms (*2*, *4*−*7*) have revealed that FeMo-cofactor is composed of a [Mo-3Fe-3S] subcluster and a [4Fe-3S] subcluster bridged by three μ_2-sulfides, with homocitrate bound to the Mo (Figure 1). A recently determined high-resolution structure of the MoFe protein has revealed the presence of an atom of unknown identity {suggested to be either N [not exchangeable (*8*)], O, or C} in the middle of FeMo-cofactor (*7*). Despite the availability of these structures, there remains a paucity of experimental data indicating the exact site on FeMo-cofactor that accommodates substrate binding, and the sequence of events occurring during substrate reduction. On the basis of studies of inorganic compounds as possible mimics of FeMo-cofactor (*9*−*14*) and on the basis of calculations considering the structure of FeMo-cofactor (*15*−*27*), several different modes for substrate binding to FeMo-cofactor have been proposed, including end-on or bridging coordination with one or more Fe atoms at the waist, or with

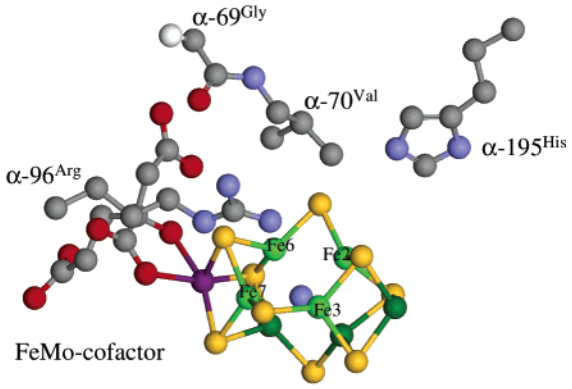

FIGURE 1: FeMo-cofactor and selected residues of the immediate protein environment. Shown are FeMo-cofactor (including homocitrate on the left) and the positions of the α-96^{Arg}, α-69^{Gly}, α-70^{Val}, and α-195^{His} residues of the *A. vinelandii* MoFe protein. Fe atoms are numbered as previously assigned (*5*). Figures were generated from the coordinates for the MoFe protein [PDB entry 1M1N (*7*)] using the program Discovery Studio Viewer Pro 5.0. Atom colors are as follows: carbon in gray, nitrogen in blue, molybdenum in magenta, sulfur in yellow, and iron in green. The identity of the atom in the center of FeMo-cofactor (shown in blue) is not known, but has been suggested to be N, C, or O.

† This work was supported by National Institutes of Health Grant R01-GM59087 (to L.C.S. and D.R.D.) and National Science Foundation Grant MCB-9904018 (to B.M.H.).

* To whom correspondence should be addressed. L.C.S.: phone, (435) 797-3964; fax, (435) 797-3390; e-mail, seefeldt@cc.usu.edu. D.R.D.: phone, (540) 231-5895; fax, (540) 231-7126; e-mail, deandr@vt.edu. B.M.H.: phone, (847) 491-3104; fax, (847) 491-7713; e-mail, bmh@northwestern.edu.

‡ Utah State University.

§ Northwestern University.

|| Virginia Tech.

[1] Abbreviations: Fe protein, iron protein; MoFe protein, molybdenum−iron protein; FeMo-cofactor, iron−molybdenum cofactor; EPR, electron paramagnetic resonance; ENDOR, electron nuclear double resonance.

10.1021/bi034595x CCC: $25.00
Published on Web 07/11/2003

the Mo. Recent spectroscopic studies on nitrogenase proteins trapped during turnover in the presence of the inhibitor CO (*28*−*30*) or the substrates CS_2 (*31*) and acetylene (*32*−*34*) point to one or more Fe atoms as being the likely site for binding these molecules, but there is no information about which of the Fe atoms are involved.

It is clear that the protein environment around FeMo-cofactor provided by the MoFe protein plays an integral role in defining the reactivity of FeMo-cofactor (*35*), and likely in defining specifically which Fe atoms are involved in binding specific substrates (*36*). A critical role for the protein is indicated by the observation that FeMo-cofactor can be extracted into organic solvents (*1*), but this isolated cofactor lacks the reactivity of the cofactor bound to the protein (*37*). In further support are the observations that changing certain amino acid residues of the MoFe protein comprising the first shell around FeMo-cofactor can alter various aspects of the reactivity of the enzyme (*35*). Recently, we have been investigating the roles of several amino acids in the MoFe protein located near one of three [4Fe-4S] faces of FeMo-cofactor (comprised of Fe atoms 2, 3, 6, and 7 and S atoms 2A, 2B, 3B, and 5) in defining nitrogenase reactivity (Figure 1). Among our findings is that substituting α-96^{Arg} near this face with several other amino acids exposes the FeMo-cofactor for binding of acetylene or cyanide in the absence of turnover conditions (*32*). Normally, substrate interactions with FeMo-cofactor are only observed during turnover, which requires functioning Fe protein delivering electrons to the MoFe protein. This requirement for turnover conditions suggests that substrate access to FeMo-cofactor is regulated by movement of amino acids to expose FeMo-cofactor and/or by changes in the reactivity of FeMo-cofactor. Substitution of α-96^{Arg} with other amino acids apparently can at least partially simulate the turnover-dependent changes that are required for substrate binding. We have also found that substitution of α-70^{Val} near this face with Ala or Gly expands the substrate range of nitrogenase (*38*). Normally, nitrogenase reduces a family of relatively small molecules containing double and triple bonds such as N_2 or acetylene (*39*). Larger alkynes, such as propyne and butyne, are very poor substrates (*39*). Substitution of α-70^{Val} with amino acids with smaller side chains (Ala and Gly) results in MoFe proteins that are able to reduce the larger alkynes propyne, propargyl alcohol ($HC{\equiv}CCH_2OH$), and 1-butyne at significant rates (*38*). Last, substitution of α-195^{His} on this face with His or Asn has been shown to alter several aspects of substrate reduction by nitrogenase (*33*, *34*, *40*−*43*).

Taken together, these studies point to one [4Fe-4S] face of FeMo-cofactor as the likely binding site for at least some nitrogenase substrates and further suggest specific roles for individual amino acids near this face in tuning the reactivity of FeMo-cofactor. Here we report evidence for direct binding of propargyl alcohol to FeMo-cofactor in an α-70^{Ala} MoFe protein trapped during turnover. X- and Q-band EPR and Q-band ENDOR spectroscopies are used to characterize this substrate-bound state of the MoFe protein. These results, coupled with the observation that propargyl alcohol only becomes a substrate when α-70^{Val} is substituted, localize the binding site for this substrate at the adjacent [4Fe-4S] face of FeMo-cofactor. These results also indicate a role for α-70^{Val} in controlling access of substrates to FeMo-cofactor.

EXPERIMENTAL PROCEDURES

Protein Purification and Activity Assays. Construction of an *Azotobacter vinelandii* strain (DJ1310) expressing the α-70^{Ala} variant MoFe protein was previously described (*38*). Wild-type (α-70^{Val}) and α-70^{Ala} MoFe proteins containing a polyhistidine tag were expressed in *A. vinelandii* cells and purified to homogeneity as previously described (*44*). The wild-type Fe protein was expressed and purified as described previously (*45*). The specific activity for C_2H_2 reduction catalyzed by wild-type nitrogenase proteins was ~2000 nmol of product min^{-1} (mg of protein)$^{-1}$. All protein manipulations were conducted in the absence of oxygen in septum-sealed serum vials under an argon atmosphere. All anaerobic liquid and gas transfers were performed using gastight syringes. Acetylene reduction assays were performed as previously described (*46*).

Preparation of Turnover and Nonturnover MoFe Protein EPR Samples. Nitrogenase samples under turnover conditions were prepared in a solution of 100 mM MOPS buffer (pH 7.0) that contained 80 μM MoFe protein, 35 mM sodium dithionite ($Na_2S_2O_4$), 10 mM ATP, 20 mM phosphocreatine, 15 mM $MgCl_2$, 75 μg/mL creatine phosphokinase, and 0.5 mg/mL bovine serum albumin under 1 atm of Ar. The reaction was initiated by the addition of wild-type Fe protein (40 μM) followed by incubation at 25 °C for 45 s. A sample (250 μL) was removed and transferred into a septum-sealed, Ar-filled 4 mm quartz EPR tube and immediately frozen in liquid nitrogen. Nonturnover (resting-state) MoFe protein samples (80 μM) were prepared in 100 mM MOPS buffer (pH 7.0) that contained 35 mM sodium dithionite and were under 1.0 atm of Ar. Unless stated otherwise, the initial concentration of propargyl alcohol ($HC{\equiv}CCH_2OH$) was 10 mM. A 0.1 M stock solution of propargyl alcohol was prepared by adding a predetermined volume of neat propargyl alcohol (Aldrich, Milwaukee, WI) to an appropriate volume of 100 mM MOPS buffer (pH 7.0). Samples with CO were prepared by equilibrating the sample under the desired partial pressure of CO prior to initiating the turnover reaction.

The reversibility of the propargyl alcohol-dependent EPR changes was assessed by passing an appropriately treated MoFe protein sample through a Sephadex G-25 column equilibrated with 50 mM Tris buffer (pH 8.0) with 300 mM NaCl and 2 mM dithionite. The resulting protein solution was transferred immediately to a septum-sealed EPR tube and frozen in liquid nitrogen.

Samples for ^{13}C ENDOR were prepared with an MoFe protein concentration of 240 μM and an Fe protein concentration of 120 μM. ^{12}C- or ^{13}C-labeled (Cambridge Isotopes, Andover, MA) propargyl alcohol was added at an initial concentration of 10 mM.

EPR and ENDOR Spectroscopy. X-band EPR spectroscopy was performed using a Bruker ESP-300E spectrometer equipped with an ER 4116 DM dual-mode X-band cavity and an Oxford Instruments ESR-900 helium flow cryostat. In all cases, calibrated quartz EPR tubes (Wilmad, Buena, NJ) were used. Independently recorded background spectra of the cavity were aligned with and subtracted from experimental spectra. EPR spectra were recorded at a modulation frequency of 100 kHz and a modulation amplitude of 1.26 mT (12.6 G) with a sweep rate of 10 mT/s. X-band EPR spectra were recorded at microwave frequencies

of approximately 9.64 GHz, with the precise microwave frequencies recorded for individual spectra to ensure exact *g* alignment. Unless stated otherwise, all spectra were recorded at a temperature of 5 K and a microwave power of 2.0 mW, and each trace represents the sum of five scans. Subsequent manipulations of spectral data (including the generation of all graphical representations) were accomplished using the program Igor Pro (WaveMetrics, Lake Oswego, OR). Spin integration of EPR signals was accomplished by comparison to the integrated area for the wild-type FeMo-cofactor $S = {}^3/_2$ signal.

Q-Band (35.287 GHz) EPR and ENDOR spectra were recorded on a modified Varian E-110 ENDOR capable continuous-wave (cw) spectrometer, at 2 K in dispersion mode, using a field modulation of 100 kHz under "rapid passage" conditions as described previously (*47*). Mims-pulsed ENDOR spectra were taken on a lab-built spectrometer, as described previously (*48*). The spectrum for ^{13}C with a hyperfine coupling (*A*) is a doublet centered at the ^{13}C Larmor frequency and split by *A* (*49*) in a Mims-pulsed ENDOR spectrum, when *A* and τ satisfy the relation $A\tau = n$ (0, 1, 2, ...), the intensity for a particular hyperfine coupling, *A*, is suppressed, creating a so-called "Mims suppression hole" (*50*).

Temperature and Power Dependence of EPR Signals. For the temperature dependence of EPR signals, the nonsaturating microwave power at 5 K was established for each MoFe protein sample from plots of EPR signal intensity versus the square root of the microwave power. These values were 1.0 mW for the wild-type turnover and nonturnover MoFe protein samples, 0.4 mW for the wild-type MoFe protein under turnover conditions with lo CO, and 0.8 mW for the α-70^{Ala} MoFe protein under turnover conditions with propargyl alcohol. X-Band EPR spectra were then recorded for each sample at the optimal nonsaturating microwave power at different temperatures. The peak height for the relevant EPR signal was plotted against the temperature, and the data were fit to either (i) the equation describing Curie law $1/T$ dependence (eq 1)

$$S = k/T + x \quad (1)$$

where *S* is the EPR signal intensity, *k* is an arbitrary constant, *T* is the temperature in kelvin, and *x* is a correction factor or (ii) by connecting the points.

For the microwave power dependence of the EPR signals, spectra (the sum of five scans) were acquired at 5 K and at microwave powers ranging from 0.05 to 25.3 mW. The microwave power was taken as that recorded from the bridge, and thus, the actual power at the sample may be different from that reported depending on the particular spectrometer. The relative intensity of the EPR signals was adjusted to a common value for the purposes of the graph shown in Figure 5. The data for the nonturnover sample are fit to a single exponential, while the data for the turnover samples are fit to a straight line. Such fits have no theoretical significance, but rather are used to track the data.

RESULTS

EPR Signals Associated with the Reduction of Propargyl Alcohol by a Nitrogenase α*-70-Substituted MoFe Protein.*

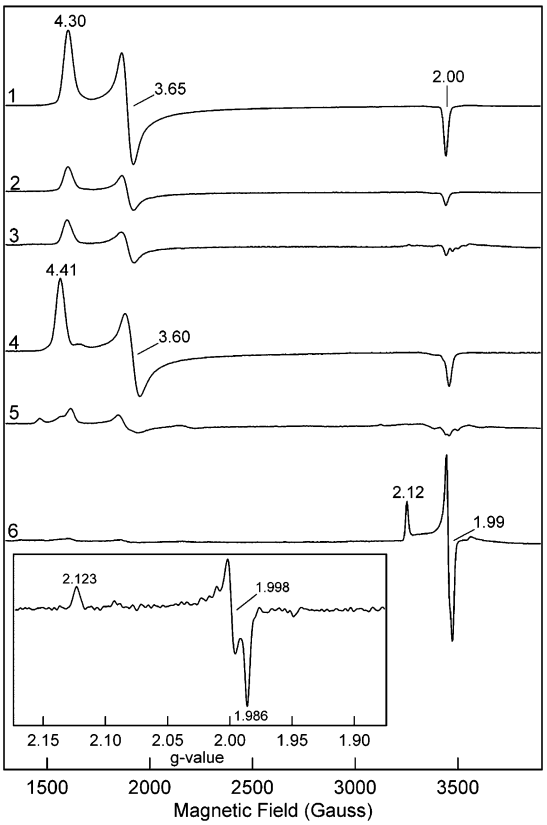

FIGURE 2: X- and Q-band EPR spectra of wild-type nitrogenase and α-70^{Ala} MoFe proteins. Wild-type (traces 1−3) and α-70^{Ala} (traces 4−6) MoFe proteins were prepared under the following conditions: nonturnover conditions under 1.0 atm of Ar (traces 1 and 4), turnover conditions under 1.0 atm of Ar (traces 2 and 5), and turnover conditions under 1 atm of Ar with 10 mM propargyl alcohol (traces 3 and 6). Sample preparation and EPR parameters are described in Experimental Procedures. The inset shows the Q-band EPR spectrum for the α-70^{Ala} MoFe protein trapped during turnover with propargyl alcohol.

In the as-isolated, resting state, the MoFe protein exhibits an EPR spectrum arising from the $S = {}^3/_2$ resting state of FeMo-cofactor (M^N) (*43*−*45*) (Figure 2, trace 1). In this state, the P-clusters are in a P^N ($S = 0$) state and are EPR silent (*51*). The α-70^{Ala} MoFe protein in the resting state exhibits an $S = {}^3/_2$ EPR signal (Figure 2, trace 4) like the wild-type MoFe protein (trace 1), with small shifts in the two higher *g* values. The lack of significant perturbations of the FeMo-cofactor EPR spectrum suggests that this amino acid substitution has not significantly altered the electronic environment of FeMo-cofactor.

Under turnover conditions created by the addition of the Fe protein, MgATP, and a reductant, the MoFe protein achieves a steady state with a greatly diminished EPR intensity (*51*, *52*) (Figure 2, trace 2). This has been interpreted as a result of FeMo-cofactor being reduced to an EPR-silent state (M^R; $S \geq 1$), the P-clusters remaining in the P^N ($S = 0$) state, and the [4Fe-4S] cluster of the Fe protein being oxidized to a 2+ oxidation state ($S = 0$) (*51*). When turnover conditions come to an end (e.g., when one or more of the cosubstrates is exhausted), FeMo-cofactor is observed to relax back to the $S = {}^3/_2$ EPR signal of the resting state. The α-70^{Ala} MoFe protein behaves in a manner similar to that of the wild-type MoFe protein under turnover when protons are the substrate (compare traces 2 and 5 in Figure 2).

Given the earlier observations that the α-70^{Ala}-substituted MoFe protein can reduce the alkynes propyne and propargyl alcohol (HC≡CCH$_2$OH) at significant rates (*38*), unlike the wild-type nitrogenase, it was of interest to monitor possible changes in the EPR spectrum during turnover with these molecules. Wild-type nitrogenase trapped under turnover conditions in the presence of propyne or propargyl alcohol exhibited no significant changes in its EPR spectrum, consistent with these compounds being poor substrates (Figure 2, trace 3). In contrast, when the α-70^{Ala} variant MoFe protein was trapped during turnover with propargyl alcohol, it developed a new, intense EPR spectrum (Figure 2, trace 6). Use of propyne as a substrate instead of propargyl alcohol did not result in the development of this new EPR signal, but rather, the normal turnover state was observed (similar to trace 5 of Figure 2).

The new EPR signal observed for the α-70^{Ala} variant MoFe protein during propargyl alcohol reduction appears to be nearly axial at X-band (9.64 GHz) with a g_{parall} of 2.12 and a g_{perp} of ~2 (Figure 2, trace 6). Higher-field EPR (Q-band, 35.287 GHz) allowed the three *g* values of the rhombic signal to be resolved (g = [2.123, 1.998, 1.986]) (Figure 2, inset). Both the X- and Q-band spectra are dominated by this EPR signal, with a few other minor signals apparent. Integration of this dominant EPR signal indicates ~0.2 spin per FeMo-cofactor when compared to the resting-state FeMo-cofactor EPR signal.

The formation of the propargyl alcohol-dependent EPR signal was completely reversible as evidenced by the return of a resting-state EPR spectrum upon removal of propargyl alcohol from the sample. Finally, trapping the α-70^{Ala} MoFe protein during turnover in the presence of allyl alcohol (H$_2$C═CHCH$_2$OH), the major reduction product of propargyl alcohol (*38*), gave an EPR spectrum like the proton reduction spectrum, indicating that the new EPR signal does not result from product binding.

The effects of varying electron flux (changing the ratio of Fe protein to MoFe protein from 10:1 to 1:5) and reaction time (from 15 to 150 s) on the shape and intensity of the new EPR signal were also examined. Over the ranges of flux and time that were examined, the shape and intensity of the propargyl alcohol-dependent EPR signal did not change appreciably, indicating that the detected intermediate is formed rapidly and represents a steady state.

The intensity of the propargyl alcohol-dependent EPR signal (monitored by the g = 2.12 feature) as a function of propargyl alcohol concentration for the α-70^{Ala} MoFe protein was found to increase with propargyl alcohol concentration, reaching a maximum near 6 mM (Figure 3). This pattern closely tracks the concentration dependence of the inhibition of both N_2 and proton reduction reported previously (*38*). In both cases, the data could be fit to a simple hyperbola, indicating simple binding of a single substrate.

Characterization of the Propargyl Alcohol-Dependent EPR Signal. The line shape and *g* values for the propargyl alcohol-dependent EPR signal of the α-70^{Ala} MoFe protein are similar to those observed for the EPR signal of the wild-type MoFe protein trapped in the presence of low concentrations of the inhibitor CO (termed the "lo CO" state) (*53*). In both cases, the intermediate EPR signal is rhombic and arises from an $S = {}^1/_2$ spin state (Figure 4). Given these similarities, the microwave power dependence and temperature dependence

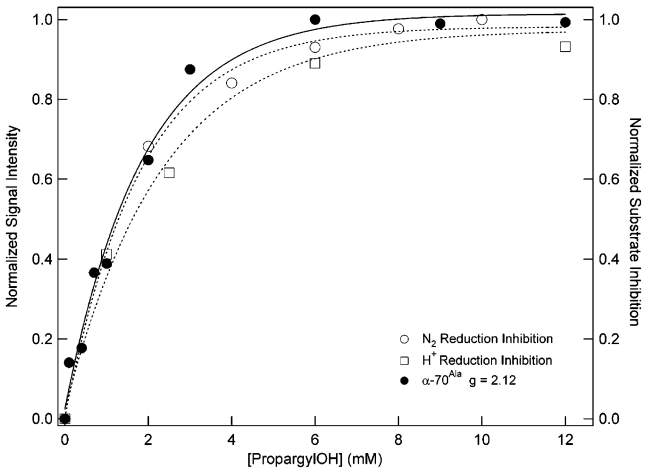

FIGURE 3: Propargyl alcohol concentration dependence. The effects of varying the propargyl alcohol concentration (from 0.1 to 12 mM) on the relative intensity (left ordinate) of the g = 2.12 EPR signal (●) and the relative inhibition (right ordinate) of H^+ (□) or N_2 (○) reduction activities are compared for the α-70^{Ala} MoFe protein under turnover conditions. Details of the EPR sample preparation and data acquisition parameters are described in Experimental Procedures. The propargyl alcohol inhibition data were adapted from Figure 3 of ref *38*. Data are fit to a single exponential.

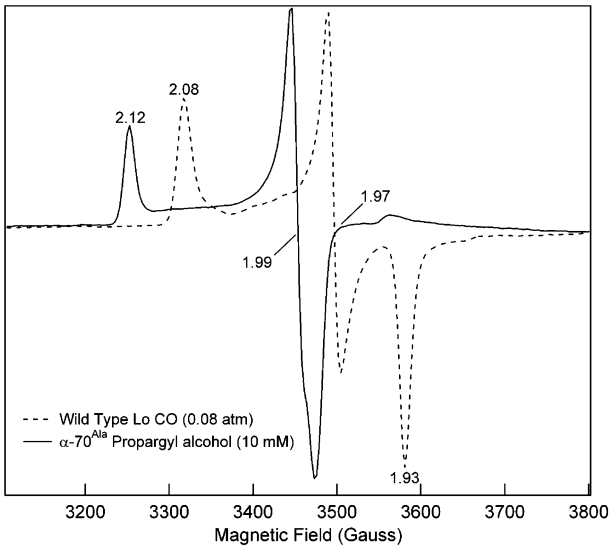

FIGURE 4: Comparison of the g ~ 2 region EPR spectra for MoFe proteins under turnover conditions. EPR spectra for the wild-type MoFe protein under turnover conditions with a partial pressure of CO of 0.08 atm (- - -) and the α-70^{Ala} MoFe protein under turnover conditions with 10 mM propargyl alcohol (—) are compared. Sample preparation and EPR parameters are described in Experimental Procedures.

of these EPR signals were determined and compared to each other and to the behavior of the EPR signal of the wild-type MoFe protein.

The microwave power dependence of EPR signals reflects the relaxation properties of the paramagnetic center. A Beinert−Orme−Johnson plot (*54*) of the dependence of the EPR signal intensities upon microwave power for various samples is shown in Figure 5. The resting-state FeMo-cofactor signal of the α-70^{Ala} variant MoFe protein shows a power dependence much like that for the wild-type FeMo-cofactor (*32*), again suggesting the absence of significant perturbations by the amino acid change. The $S = {}^1/_2$ signal from the α-70^{Ala} variant MoFe protein under turnover with

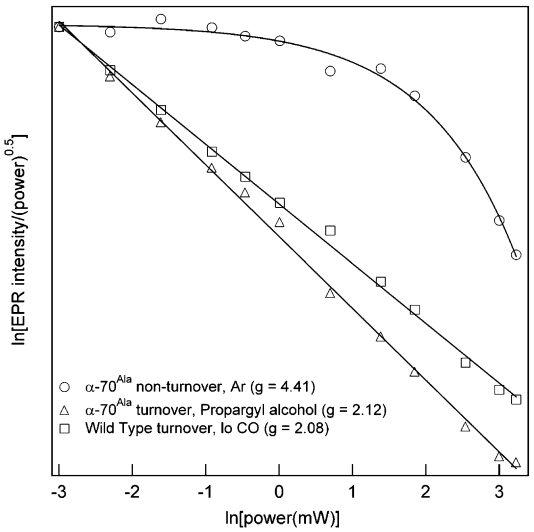

FIGURE 5: Microwave power dependence of the EPR signals for MoFe proteins. EPR signal intensities were determined at a constant temperature of 5 K, and at various microwave powers ranging from 0.1 to 25.3 mW for the $g = 4.41$ inflection of the α-70^{Ala} MoFe protein under nonturnover conditions (○), the $g = 2.12$ inflection of the α-70^{Ala} MoFe protein under turnover conditions with 10 mM propargyl alcohol (△), and the wild-type MoFe protein under turnover conditions with a CO partial pressure of 0.08 atm (□). The natural logarithm of the normalized signal intensities divided by the square root of the microwave power is plotted against the natural logarithm of the microwave power. The data for the nonturnover sample are fit to a single exponential, while the data for the turnover samples are fit to a straight line. Sample preparation and other EPR parameters are described in Experimental Procedures.

propargyl alcohol showed microwave saturation at a much lower microwave power when compared to the wild-type FeMo-cofactor signal, as does the $S = {}^1/_2$ lo CO signal from the wild-type MoFe protein.

The temperature dependence of the EPR signal intensities is shown in Figure 6. The intensity of the resting-state FeMo-cofactor EPR signal in the wild-type MoFe protein declines with increasing temperature from 4 to 30 K, roughly following a Curie law $1/T$ dependence, consistent with a ground-state transition. The temperature dependence of the propargyl alcohol-dependent signal in the α-70^{Ala} MoFe protein increases in intensity upon going from 4 to ~10 K and then declines in intensity upon going from 10 to 30 K. The lo CO EPR signal for wild-type FeMo-cofactor behaves like the propargyl alcohol-dependent signal.

^{13}C ENDOR. ENDOR spectroscopy was used to determine if propargyl alcohol binds directly to the paramagnetic center giving rise to the $S = {}^1/_2$ turnover EPR signal. Figure 7 presents the single-crystal-like cw ENDOR spectrum taken at a g_3 of 1.99 for the α-70^{Ala} MoFe protein trapped during turnover with uniformly ^{13}C-labeled propargyl alcohol. The spectrum shows an intense ^{13}C doublet that is absent with the ^{12}C substrate; it is centered at the Larmor frequency and exhibits a ^{13}C hyperfine coupling of ~3.2 MHz (C1) (Figure 7). The cw spectrum also exhibits a largely unresolved central feature that was not observed when ^{12}C propargyl alcohol was used. In the Mims-pulsed ENDOR spectrum, this resolves into two additional ^{13}C doublets centered at the Larmor frequency. These two doublets (denoted C2 and C3) are split by ^{13}C hyperfine coupling constants of ~1.4 and ~0.7 MHz, respectively.

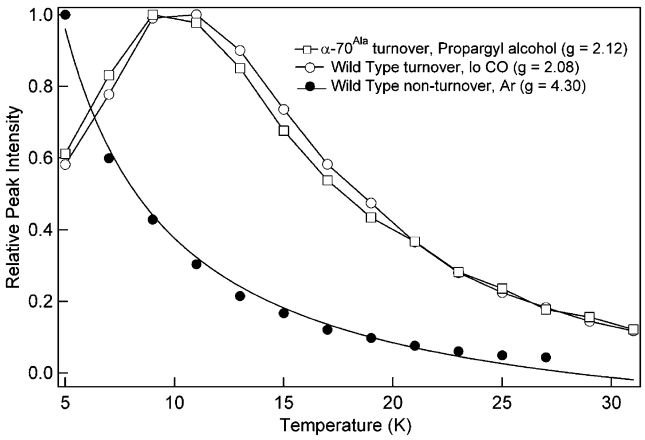

FIGURE 6: Temperature dependence of the EPR signals for MoFe proteins. EPR signal intensities were determined at various temperatures over the range from 5 to 31 K for the $g = 2.12$ inflection of the α-70^{Ala} MoFe protein under turnover conditions with 10 mM propargyl alcohol (□), the $g = 2.08$ inflection of the wild-type MoFe protein under turnover conditions under a CO partial pressure of 0.08 atm (○), and the $g = 4.30$ inflection of the wild-type MoFe protein under nonturnover conditions under 1 atm of Ar (●). Sample preparation and other EPR parameters are described in Experimental Procedures. The data for the wild-type MoFe protein under nonturnover conditions are fit to the equation for Curie law $1/T$ dependence. All other data are connected by lines between the points.

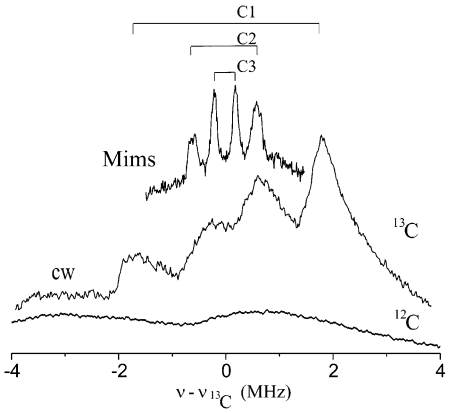

FIGURE 7: Q-band cw and Mims three-pulse ENDOR spectra of the α-70^{Ala} MoFe protein under turnover conditions with ^{12}C and ^{13}C propargyl alcohol. cw ENDOR spectra (bottom two traces) are for the α-70^{Ala} MoFe protein trapped under turnover conditions with either ^{12}C propargyl alcohol (bottom trace) or ^{13}C propargyl alcohol (second from the bottom). Q-Band cw ENDOR spectra were obtained at 2 K, a microwave frequency of 34.827 GHz, a modulation amplitude of 1.3 G, an RF power of 20 W, and an RF sweep speed of 0.5 MHz/s. Mims-pulsed ENDOR spectra (upper trace) were acquired with a three-pulse sequence [T_{mw}−tau−t_{mw}−T(rf)−t_{mw}−tau−echo] with the following: MW pulse length $t_{MW} = 52$ ns, $\tau = 600$ ns, RF pulse length = 60 μs, and repetition rate = 20 Hz. The bandwidth of the radio frequency (RF) is broadened to 100 kHz to increase the signal-to-noise ratio (*57*).

DISCUSSION

Propargyl Alcohol Binding to FeMo-Cofactor. Substitution of the MoFe protein α-70^{Val} residue with alanine permits propargyl alcohol to inhibit the reduction of other substrates (e.g., protons and N_2) and to serve as a substrate for reduction by the substituted MoFe protein (*38*). Given that the FeMo-cofactor of nitrogenase provides the active site, it was concluded that propargyl alcohol interacts with the FeMo-cofactor in this altered MoFe protein. In the work presented

here, it is demonstrated that propargyl alcohol binds to FeMo-cofactor in the α-70^{Ala} MoFe protein, forming an intermediate that can be trapped during reduction. The FeMo-cofactor-bound intermediate exhibits an $S = {}^1/_2$ EPR signal with a rhombic **g** tensor. In contrast, during turnover, the wild-type MoFe protein goes to a nearly EPR-silent state, which has been interpreted as the reduction of the FeMo-cofactor to the M^R ($S \geq 1$) state (*51*, *52*).

This new EPR signal can be compared to other signals that have been observed when substrates or inhibitors generate intermediates during turnover. The lo CO state of the wild-type MoFe protein formed during turnover under CO (*28*−*30*, *53*, *55*) and the so-called S_{EPR1} state formed by the α-195^{Gln} variant of the MoFe protein during turnover with C_2H_2 (*33*, *34*) both exhibit $S = {}^1/_2$ signals with properties similar to those of the propargyl alcohol-induced EPR signal; Figure 4 compares the EPR signals from the lo CO and propargyl alcohol intermediates. In the case of the α-195$^{His\rightarrow Gln}$ variant MoFe protein, turnover with acetylene permits the trapping of three new $S = {}^1/_2$ EPR signals in the $g \sim 2$ region (*34*). While the propargyl alcohol-induced EPR spectrum reported here has a **g** tensor similar to those of the lo CO- and acetylene-dependent signals, further comparison of properties of the species reveals important differences. For example, the EPR signal arising from the propargyl alcohol-bound state in the α-70^{Ala} MoFe protein increases in intensity upon going from 4 to ∼10 K, followed by a progressive decrease in intensity upon going from 10 to 30 K. The temperature dependence of the lo CO signal behaves in a similar way (Figure 6). This contrasts with the rapid decline in intensity observed for the acetylene-bound EPR signal in the α-195^{Gln} MoFe protein, which decreases from 4 to 8 K (*33*). The latter behavior is similar to what is observed for the resting-state FeMo-cofactor signal.

The microwave power dependence of the new EPR signal for the α-70^{Ala} MoFe protein with propargyl alcohol bound is also similar to that observed for the lo CO-bound state of FeMo-cofactor in the wild-type MoFe protein (Figure 5). In both $S = {}^1/_2$ cases, the signals are easily microwave saturatable, unlike the more rapidly relaxing, $S = 3/2$, resting-state FeMo-cofactor EPR signal. The microwave power saturation profile for the acetylene-bound state has not been reported but can be expected to follow those of the other two $S = {}^1/_2$ intermediates.

The dependence of the EPR signal intensity upon substrate concentration for propargyl alcohol also distinguishes this state from the acetylene-bound state. For propargyl alcohol, the EPR signal intensity develops over the same propargyl alcohol concentration range as does propargyl alcohol inhibition of proton or N_2 reduction. Further, the signal develops hyperbolically, indicating a single binding event. This contrasts with a sigmoidal response for acetylene concentration dependence on the development of the EPR signal in the α-195^{Gln} MoFe protein, which has been interpreted as resulting from the binding of two or more acetylene molecules (*33*). Overall, the propargyl alcohol-bound state of the α-70^{Ala} MoFe protein shares many similarities with the lo CO-bound state of the wild-type MoFe protein, while showing important differences with the acetylene-bound state of the α-195^{Gln} MoFe protein.

The observation of ^{13}C ENDOR signals when the α-70^{Ala} MoFe protein is trapped with ^{13}C-labeled propargyl alcohol, but not with ^{12}C-labeled substrate, demonstrates that propargyl alcohol is binding directly to FeMo-cofactor, and not exerting its influence on the EPR properties by binding near FeMo-cofactor. We observe a strongly coupled ^{13}C signal in the cw ENDOR spectrum, with a hyperfine coupling constant at g_3 of ∼3.2 MHz (designated C1), along with two weakly coupled ^{13}C signals seen in the pulsed ENDOR spectrum, with couplings of ∼1.4 and ∼0.7 MHz (designated C2 and C3, respectively). The presence of three distinct ^{13}C ENDOR signals can be explained in different ways. In one limit, each ^{13}C signal could arise from one carbon of a different bound propargyl alcohol. This was the case for CS_2 binding to FeMo-cofactor, where three ENDOR signals were observed and assigned to three different CS_2-bound adducts (*31*). However, the concentration dependence data for propargyl alcohol are not consistent with this model, rather suggesting the binding of a single propargyl alcohol to FeMo-cofactor. This supports the more likely possibility that each ENDOR signal represents one of the three C atoms of a single propargyl alcohol bound to the cofactor. If the terminal C of the alkyne binds to Fe, it would have the strongest coupling with progressively weaker couplings corresponding to the other two C atoms, while if the alcohol O were bound to Fe, this progression would be reversed. The hyperfine couplings reported here are in the range of values observed previously for C-containing substrates (C_2H_2, CS_2, and cyanide) (*30*−*32*, *34*) and for the inhibitor CO (*34*) bound to FeMo-cofactor. In the case of the lo CO state, which is the most similar to the propargyl alcohol-bound state, ^{57}Fe isotopomers of FeMo-cofactor were used to establish that CO is bound to (one or more) Fe atoms (*29*), rather than Mo, and it seems reasonable to conclude that propargyl alcohol is bound likewise. While we cannot rule out the involvement of Mo in binding propargyl alcohol, this seems unlikely for several reasons. The similarities with the lo CO-bound state as noted above suggest binding to Fe atoms. As the α-70^{Val} side chain resides directly over one [4Fe-4S] face of FeMo-cofactor, and reducing the size of this side chain is necessary for association of propargyl alcohol, we infer the involvement of one or more of the Fe atoms contained in this face (Figure 1). Several different modes for binding propargyl alcohol can be envisaged (Scheme 1). Detailed ENDOR studies, such as those done for bound CO and C_2H_2, in particular ^{2}H ENDOR measurements using appropriately deuterated samples, should provide a means of distinguishing among these.

Scheme 1

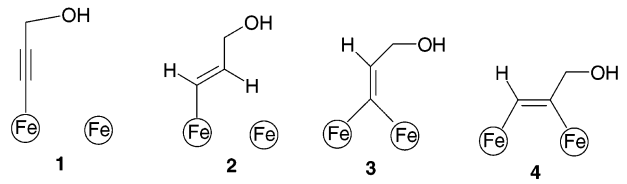

Additional information about how propargyl alcohol might bind to FeMo-cofactor comes from the observation that while propyne is a substrate for the α-70^{Ala} MoFe protein, it does not induce any significant turnover-dependent EPR signals. This suggests that the hydroxyl group of propargyl alcohol plays a role in stabilizing the bound state, possibly by interacting with amino acid residues, or possibly by binding to one or more Fe atoms of FeMo-cofactor.

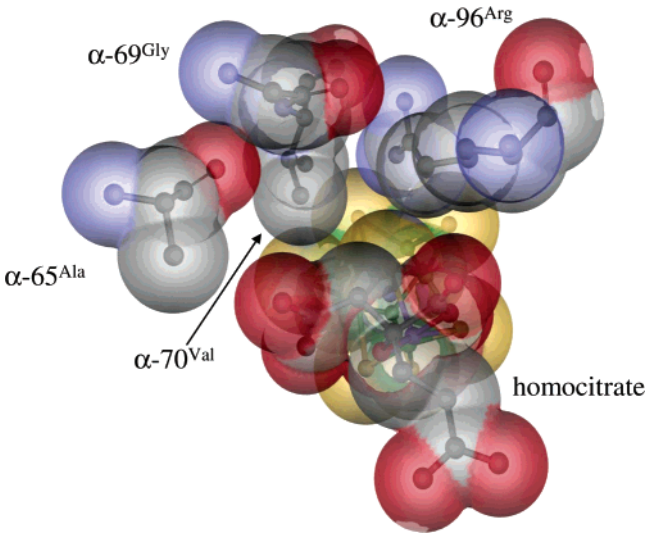

FIGURE 8: FeMo-cofactor and its protein environment. A van der Waals surface is shown for FeMo-cofactor and the MoFe protein amino acid side chains only for α-65^{Ala}, α-69^{Gly}, α-96^{Arg}, and α-70^{Val}. The view is from the homocitrate end of FeMo-cofactor, looking into the proposed substrate binding channel and substrate binding [4Fe-4S] cluster face of FeMo-cofactor. The figure was generated from the atomic coordinates for the MoFe protein [PDB entry 1M1N (*7*)] using the program Discovery Studio Viewer Pro 5.0. Relative atomic and ionic radii for individual atoms were taken from refs *58*−*60*. Atom colors are as follows: carbon in gray, oxygen in red, nitrogen in blue, molybdenum in magenta, sulfur in yellow, and iron in green.

If propargyl alcohol binds to the Fe−S face of FeMo-cofactor defined by Fe atoms 2, 3, 6, and 7 (Figure 1), where might other substrates bind? We favor a model whereby all substrate bind at the same [4Fe-4S] face, albeit to different oxidation states of FeMo-cofactor. Propargyl alcohol competes for electrons when N_2 or protons are substrates (*38*). Further, acetylene and N_2 binding and reduction are competitive in an α-69^{Ser} variant MoFe protein (*36*, *56*), indicating that these two substrates bind to the same site on FeMo-cofactor. Earlier kinetic studies clearly point to different substrates binding to different oxidation states of FeMo-cofactor, with N_2 requiring a more reduced state (by at least three electrons) compared to the state necessary to bind acetylene.

Role for α-70^{Val} in the MoFe Protein. Last, the observation that propargyl alcohol only becomes a substrate when α-70^{Val} is substituted with amino acids with smaller side chains suggests that this side chain controls reactivity in part by restricting access of substrates to the active site. As can be seen in Figure 8, the [4Fe-4S] face of FeMo-cofactor that we propose as the active site is partially shielded by the side chain of α-70^{Val}. Thus, substituting α-70^{Val} with Ala might be expected to allow access of the larger alkyne to the [4Fe-4S] face shielded by this residue. It is interesting to note, however, that substituting α-70^{Val} with Ala is not sufficient to allow smaller substrates such as acetylene to bind in the resting state, as was observed when the α-96^{Arg} side chain was changed to amino acids with smaller side chains (*32*). This suggests that changes in the position of α-96^{Arg} are induced by the reduction of FeMo-cofactor and are required for substrate binding.

In summary, the results presented here are consistent with the [4Fe-4S] face of FeMo-cofactor that is capped by α-70^{Val} and α-96^{Arg} providing the initial binding site for the substrate propargyl alcohol. It seems likely that this face also provides the site for binding other substrates (e.g., N_2 and acetylene) and inhibitors (e.g., CO). Also consistent with the results presented here is a role for the side chain of α-70^{Val} in providing a steric limitation to the size of substrates that can access the proposed active site [4Fe-4S] face.

ACKNOWLEDGMENT

We thank Dr. Brian Bennett of the Medical College of Wisconsin for assistance with EPR data analysis.

REFERENCES

1. Shah, V. K., and Brill, W. J. (1977) *Proc. Natl. Acad. Sci. U.S.A. 74*, 3249−3253.
2. Kim, J., and Rees, D. C. (1992) *Science 257*, 1677−1682.
3. Shah, V. K., Davis, I. C., Gordon, J. K., Orme-Johnson, W. H., and Brill, W. J. (1973) *Biochim. Biophys. Acta 292*, 246−255.
4. Kim, J., Woo, D., and Rees, D. C. (1993) *Biochemistry 32*, 7104−7115.
5. Kim, J., and Rees, D. C. (1992) *Nature 360*, 553−560.
6. Mayer, S. M., Lawson, D. M., Gormal, C. A., Roe, S. M., and Smith, B. E. (1999) *J. Mol. Biol. 292*, 871−891.
7. Einsle, O., Tezcan, F. A., Andrade, S. L. A., Schmid, B., Yoshida, M., Howard, J. B., and Rees, D. C. (2002) *Science 297*, 1696−1700.
8. Lee, H. I., Benton, P. M., Laryukhin, M., Igarashi, R. Y., Dean, D. R., Seefeldt, L. C., and Hoffman, B. M. (2003) *J. Am. Chem. Soc. 125*, 5604−5605.
9. Lehnert, N., Wiesler, B. E., Tuczek, F., Hennige, A., and Sellmann, D. (1997) *J. Am. Chem. Soc. 119*, 8869−8878.
10. Malinak, S. M., Simeonov, A. M., Mosier, P. E., McKenna, C. E., and Coucouvanis, D. (1997) *J. Am. Chem. Soc. 119*, 1662−1667.
11. Malinak, S. M., and Coucouvanis, D. (2001) *Prog. Inorg. Chem. 49*, 599−662.
12. Coucouvanis, D., Han, J., and Moon, N. (2002) *J. Am. Chem. Soc. 124*, 216−224.
13. Sellmann, D., and Sutter, J. (1997) *Acc. Chem. Res. 30*, 460−469.
14. Osterloh, F., Achim, C., and Holm, R. H. (2001) *Inorg. Chem. 40*, 224−232.
15. Deng, H., and Hoffmann, R. (1993) *Angew. Chem., Int. Ed. Engl. 32*, 1062−1065.
16. Dance, I. (1996) *J. Biol. Inorg. Chem. 1*, 581−586.
17. Siegbahn, P. E. M., and Blomberg, M. R. A. (1999) *Annu. Rev. Phys. Chem. 50*, 221−249.
18. Barriere, F., Pickett, C. J., and Talarmin, J. (2001) *Polyhedron 20*, 27−36.
19. Pickett, C. J. (1996) *J. Biol. Inorg. Chem. 1*, 601−606.
20. Stavrev, K. K., and Zerner, M. C. (1998) *Int. J. Quantum Chem. 70*, 1159−1168.
21. Rod, T. H., and Norskov, J. K. (2000) *J. Am. Chem. Soc. 122*, 12751−12763.
22. Lovell, T., Li, J., Liu, T., Case, D. A., and Noodleman, L. (2001) *J. Am. Chem. Soc. 123*, 12392−12410.
23. Durrant, M. C. (2002) *Biochemistry 41*, 13934−13945.
24. Durrant, M. C. (2002) *Biochemistry 41*, 13946−13955.
25. Hinnemann, B., and Norskov, J. K. (2003) *J. Am. Chem. Soc. 125*, 1466−1467.
26. Lovell, T., Liu, T., Case, D. A., and Noodleman, L. (2003) *J. Am. Chem. Soc. 125*, 8377−8383.
27. Dance, I. (2003) *Chem. Commun.*, 324−325.
28. Pollock, C. R., Lee, H.-I., Cameron, L. M., DeRose, V. J., Hales, B. J., Orme-Johnson, W. H., and Hoffman, B. M. (1995) *J. Am. Chem. Soc. 117*, 8686−8687.
29. Christie, P. D., Lee, H. I., Cameron, L. M., Hales, B. J., Orme-Johnson, W. H., and Hoffman, B. M. (1996) *J. Am. Chem. Soc. 118*, 8707−8709.
30. Lee, H. I., Cameron, L. M., Hales, B. J., and Hoffman, B. M. (1997) *J. Am. Chem. Soc. 119*, 10121−10126.
31. Ryle, M. J., Lee, H. I., Seefeldt, L. C., and Hoffman, B. M. (2000) *Biochemistry 39*, 1114−1119.

32. Benton, P. M. C., Mayer, S. M., Shao, J., Hoffman, B. M., Dean, D. R., and Seefeldt, L. C. (2001) *Biochemistry 40*, 13816−13825.
33. Sørlie, M., Christiansen, J., Lemon, B. J., Peters, J. W., Dean, D. R., and Hales, B. J. (2001) *Biochemistry 40*, 1540−1549.
34. Lee, H. I., Sorlie, M., Christiansen, J., Song, R., Dean, D. R., Hales, B. J., and Hoffman, B. M. (2000) *J. Am. Chem. Soc. 122*, 5582−5587.
35. Christiansen, J., Dean, D. R., and Seefeldt, L. C. (2001) *Annu. Rev. Plant Physiol. Plant Mol. Biol. 52*, 269−295.
36. Christiansen, J., Seefeldt, L. C., and Dean, D. R. (2000) *J. Biol. Chem. 275*, 36104−36107.
37. Smith, B. E., Durrant, M. C., Fairhurst, S. A., Gormal, C. A., Gronberg, K. L. C., Henderson, R. A., Ibrahim, S. K., Le Gall, T., and Pickett, C. J. (1999) *Coord. Chem. Rev. 185−186*, 669−687.
38. Mayer, S. M., Niehaus, W. G., and Dean, D. R. (2002) *J. Chem. Soc., Dalton Trans.*, 802−807.
39. Burgess, B. K. (1985) in *Metal Ions in Biology: Molybdenum Enzymes* (Spiro, T. G., Ed.) pp 161−220, John Wiley and Sons, New York.
40. Dilworth, M. J., Fisher, K., Kim, C. H., and Newton, W. E. (1998) *Biochemistry 37*, 17495−17505.
41. Fisher, K., Dilworth, M. J., and Newton, W. E. (2000) *Biochemistry 39*, 15570−15577.
42. Kim, C. H., Newton, W. E., and Dean, D. R. (1995) *Biochemistry 34*, 2798−2808.
43. Thomann, H., Bernardo, M., Newton, W. E., and Dean, D. R. (1991) *Proc. Natl. Acad. Sci. U.S.A. 88*, 6620−6623.
44. Christiansen, J., Goodwin, P. J., Lanzilotta, W. N., Seefeldt, L. C., and Dean, D. R. (1998) *Biochemistry 37*, 12611−12623.
45. Burgess, B. K., Jacobs, D. B., and Stiefel, E. I. (1980) *Biochim. Biophys. Acta 614*, 196−209.
46. Seefeldt, L. C. (1994) *Protein Sci. 3*, 2073−2081.
47. Werst, M. M., Davoust, C. E., and Hoffman, B. M. (1991) *J. Am. Chem. Soc. 113*, 1533−1538.
48. Davoust, C. E., Doan, P. E., and Hoffman, B. M. (1996) *J. Magn. Reson. 119*, 38−44.
49. Abragam, A., and Bleany, B. (1986) *Electron Paramagnetic Resonance of Transition Ions*, Dover Publications, New York.
50. Schweiger, A., and Jeschke, G. (2001) *Principles of Pulse Electron Paramagnetic Resonance*, Oxford University Press, Oxford, U.K.
51. Zimmermann, R., Münck, E., Brill, W. J., Shah, V. K., Henzl, M. T., Rawlings, J., and Orme-Johnson, W. H. (1978) *Biochim. Biophys. Acta 537*, 185−207.
52. Huynh, B. H., Henzl, M. T., Christner, J. A., Zimmermann, R., Orme-Johnson, W. H., and Munck, E. (1980) *Biochim. Biophys. Acta 623*, 124−138.
53. Davis, L. C., Henzl, M. T., Burris, R. H., and Orme-Johnson, W. H. (1979) *Biochemistry 18*, 4860−4869.
54. Beinert, H., and Orme-Johnson, W. H. (1967) in *Magnetic Resonance in Biological Systems* (Ehrenberg, A., Malmstrom, B. G., and Vanngard, T., Eds.) pp 221−247, Pergamon Press, New York.
55. Cameron, L. M., and Hales, B. J. (1998) *Biochemistry 37*, 9449−9456.
56. Christiansen, J., Cash, V. L., Seefeldt, L. C., and Dean, D. R. (2000) *J. Biol. Chem. 275*, 11459−11464.
57. Hoffman, B. M., DeRose, V. J., Ong, J.-L., and Davoust, C. E. (1994) *J. Magn. Reson., Ser. A 110*, 52−57.
58. Shannon, R. D. (1976) *Acta Crystallogr. A32*, 751−767.
59. Shannon, R. D., and Prewitt, C. T. (1969) *Acta Crystallogr. B25*, 925−945.
60. Shannon, R. D., and Prewitt, C. T. (1970) *Acta Crystallogr. B26*, 1046−1048.

BI034595X